



# III/V-on-lithium niobate amplifiers and lasers

CAMIEL OP DE BEECK,<sup>1,†</sup> FELIX M. MAYOR,<sup>2,†</sup> STIJN CUYVERS,<sup>1</sup> STIJN POELMAN,<sup>1</sup> JASON F. HERRMANN,<sup>2</sup> OKAN ATALAR,<sup>2</sup> TIMOTHY P. MCKENNA,<sup>2</sup> BAHAWAL HAQ,<sup>1</sup> WENTAO JIANG,<sup>2</sup> JEREMY D. WITMER,<sup>2</sup> GUNTHER ROELKENS,<sup>1</sup> AMIR H. SAFAVI-NAEINI,<sup>2</sup> RAPHAËL VAN LAER,<sup>1,2,3</sup> AND BART KUYKEN<sup>1,\*</sup>

<sup>1</sup>Photonics Research Group, Department of Information Technology (INTEC), Ghent University-imec, Ghent, Belgium

<sup>2</sup>Department of Applied Physics and Ginzton Laboratory, Stanford University, Stanford, California 94305, USA

<sup>3</sup>Current address: Department of Microtechnology and Nanoscience, Chalmers University of Technology, Gothenburg, Sweden

\*Corresponding author: Bart.Kuyken@UGent.be

Received 5 August 2021; revised 26 August 2021; accepted 27 August 2021 (Doc. ID 438620); published 1 October 2021

**We demonstrate electrically pumped, heterogeneously integrated lasers on thin-film lithium niobate, featuring electro-optic wavelength tunability.** © 2021 Optical Society of America under the terms of the [OSA Open Access Publishing Agreement](https://doi.org/10.1364/OPTICA.438620)

<https://doi.org/10.1364/OPTICA.438620>

Lithium niobate (LN) has long been the material of choice in tele- and datacom settings for fast modulation due to its attractive electro-optic (EO) properties. However, until recently, it suffered from a lack of high-density scaling possibilities in comparison with the silicon and silicon nitride photonic platforms. Despite early attempts to address this [1], realizing both strong optical confinement and low losses simultaneously seemed out of reach in LN. In addition, while silicon and silicon nitride photonics have quickly gained scientific prominence as well as a commercial foothold, these platforms are held back by the lack of a strong second-order nonlinearity. Carrier-based modulators in silicon are indeed reaching physical performance limits [2].

The recent availability of thin-film LN (TFLN) has triggered a renewed interest in this material system, which now boasts low propagation losses, and a rapid development towards (150 nm) wafer-scale processing [3]. The TFLN platform is the result of a consistent push towards stronger confinement of the optical mode to make devices smaller and boost the efficiency of EO and all-optical interactions. Nowadays, state-of-the-art modulators with bandwidths exceeding 100 GHz are based on TFLN [4].

Light generation using optically pumped erbium-doped LN has been demonstrated previously [5], but electrically injected light sources and detectors were still missing on this platform. The heterogeneous integration of III/V gain materials on TFLN has been anticipated to fill this gap [3], and is now demonstrated in this work. Electrically injected III/V materials can offer a high gain per unit length, aiding dense integration. In addition, lasers integrated on TFLN can profit from the Pockels effect for the generation of EO-tunable frequency combs [6], to generate visible or mid-infrared light from a 1550 nm pump, or to achieve pure and fast frequency tuning for, e.g., frequency-modulated continuous-wave LiDAR. Apart from being orders of magnitude faster, EO wavelength tuning also consumes significantly less power than the

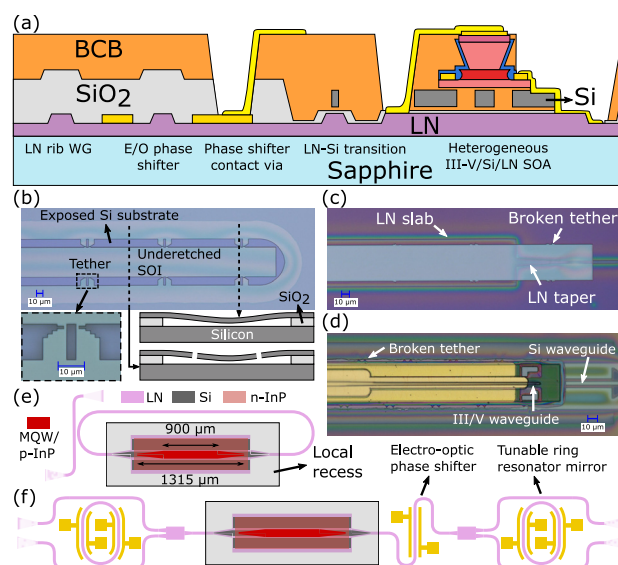


**Fig. 1.** (a) Schematic cross sections of the platform. (b) Released Si coupon on the source wafer and schematic cross section. (c) Si coupon after  $\mu$ TP on the target. (d) III/V SOA coupon after  $\mu$ TP on the Si coupon. (e) Design of III/V-on-LN ring laser. (f) Design of the single-mode tunable laser.

heaters commonly used for wavelength tuning on silicon or silicon nitride.

We developed a back-end compatible process to heterogeneously integrate III/V amplifiers onto LN waveguides. We present the first demonstration of gain, lasing, and EO wavelength tuning on this platform. A schematic drawing of the different cross sections in the platform is shown in Fig. 1(a). The starting point is a sample with 500 nm  $x$ -cut LN on top of a sapphire substrate [7]. Rib waveguides are defined using electron-beam lithography and argon milling. Metal electrodes are added on the partially etched LN layer to allow for EO phase shifting. Finally, a 1.3  $\mu$ m thick silicon oxide top cladding is deposited on the sample. Around the transfer-printing site, a local recess is etched into the top cladding down to the LN waveguide layer, ensuring that the propagation losses in the rest of the circuit are not compromised. A 400 nm

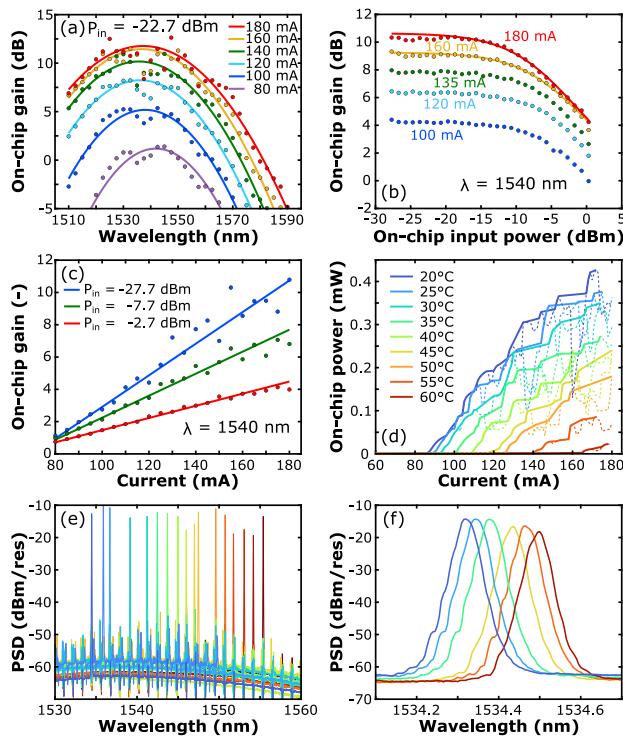


**Fig. 2.** (a) Gain bandwidth of the III/V-on-LN amplifier. (b) Gain saturation versus bias current. (c) Gain compression versus on-chip input power, linear scale. (d) LI curves of the ring laser at different temperatures. (e) Coarse wavelength tuning. (f) Fine wavelength tuning.

thick coupon of crystalline silicon (Si) is microtransfer-printed ( $\mu$ TP) on the LN in the recess, and patterned. Afterwards, a III/V semiconductor optical amplifier (SOA) is microtransfer-printed onto the silicon waveguide. Microscope images of the different parts of this process are shown in Figs. 1(b)–1(d). The post-processing steps for the electrical contacting and more details of the SOA can be found in previously reported work [8].

Three types of first-generation devices have been fabricated: optical amplifiers, multimode ring lasers, and single-mode tunable lasers. Schematic drawings of the laser designs are shown in Figs. 1(e) and 1(f). The ring laser simply connects the outputs of the amplifier, with a directional coupler extracting 10% of the circulating power each round trip. The single-mode tunable laser features an electro-optically tunable ring resonator mirror on either side of the amplifier, and an EO phase tuning section for the fine-tuning of the round trip phase. The electrodes in the rings are 324  $\mu$ m long. Figures 2(a)–2(c) show the characterization of the III/V-on-LN amplifier. From the fitted curves, a maximal gain of 11.8 dB is obtained at 1537 nm for a bias current of 180 mA. The 3 dB bandwidth of the gain at 180 mA spans over 45 nm. The gain remains linear at the measured bias current levels, with no visible thermal roll-off. When the input power reaches 160  $\mu$ W, the gain at 180 mA is reduced by 3 dB relative to the small-signal gain. The LI curves at different temperatures of the counterclockwise (CCW)

propagating mode of the ring laser are shown in Fig. 2(d). Lasing is possible up to 60°C with an output power reducing from 427  $\mu$ W at 20°C to 23  $\mu$ W. Considering the fraction of the light that is coupled out of the cavity, the on-chip CCW output power of the amplifier in the ring is 4.3 mW. The dashed lines represent the actual measured power, in which the trend is clouded due to mode hopping. For clarity, the monotonously increasing envelope of the data is highlighted by full lines. The coarse and fine tuning of the single-mode laser is shown in Figs. 2(e) and 2(f). Coarse EO wavelength tuning is shown in a wavelength range of 21 nm, whereas fine-tuning is shown in a range of 180 pm (or 22.5 GHz). This fine-tuning range is the result of a change in the bias voltage over the ring mirrors of 26 V, corresponding to a  $V_{\pi}L$  of 5.15 V  $\cdot$  cm. The highest recorded output power of the single-mode laser is 0.77 mW. Fundamental linewidths below 1.5 MHz have been measured at several operating points by heterodyning with an external laser.

We have demonstrated the first electrically pumped amplifiers and lasers integrated on a TFLN platform. The integration process of the amplifier was done entirely in the back end. The combination of electrically pumped optical gain and a strong second-order susceptibility on a single chip facilitates the development of fully integrated devices for microwave photonics, integrated quantum photonics, and nonlinear optics.

**Funding.** National Science Foundation (DGE-1656518); U.S. Department of Energy (DE-SC0019174); Air Force Office of Scientific Research (MURI No. FA9550-17-1-0002); Interreg (SAFESIDE); European Research Council (ELECTRIC); Fonds Wetenschappelijk Onderzoek (11F8120N, 1554418N).

**Disclosures.** The authors declare no conflicts of interest.

**Data availability.** Data underlying the results presented in this paper are not publicly available at this time but may be obtained from the authors upon reasonable request.

<sup>†</sup>These authors contributed equally to this work.

## REFERENCES

- J. Kondo, K. Aoki, A. Kondo, T. Ejiri, Y. Iwata, A. Hamajima, T. Mori, Y. Mizuno, M. Imaeda, Y. Kozuka, O. Mitomi, and M. Minakata, *IEEE Photon. Technol. Lett.* **17**, 2077 (2005).
- A. Rahim, A. Hermans, B. Wohlfeil, D. Petousi, B. Kuyken, D. Van Thourhout, and R. Baets, *Adv. Photon.* **3**, 1 (2021).
- M. Zhang, C. Wang, P. Kharel, D. Zhu, and M. Lončar, *Optica* **8**, 652 (2021).
- C. Wang, M. Zhang, X. Chen, M. Bertrand, A. Shams-Ansari, S. Chandrasekhar, P. Winzer, and M. Lončar, *Nature* **562**, 101 (2018).
- W. Sohler, B. K. Das, D. Dey, S. Reza, H. Suche, and R. Ricken, *IEICE Trans. Electron.* **E88-C**, 990 (2005).
- M. Zhang, B. Buscaino, C. Wang, A. Shams-Ansari, C. Reimer, R. Zhu, J. M. Kahn, and M. Lončar, *Nature* **568**, 373 (2019).
- T. P. McKenna, J. D. Witmer, R. N. Patel, W. Jiang, R. Van Laer, P. Arrangoiz-Arriola, E. A. Wollack, J. F. Herrmann, and A. H. Safavi-Naeini, *Optica* **7**, 1737 (2020).
- C. Op de Beeck, B. Haq, L. Elsinger, A. Gocalinska, E. Pelucchi, B. Corbett, G. Roelkens, and B. Kuyken, *Optica* **7**, 386 (2020).